



**HAL**  
open science

# Marker effect p-values for single-step GWAS with the algorithm for proven and young in large genotyped populations

Natália Galoro Leite, Matias Bermann, Shogo Tsuruta, Ignacy Misztal, Daniela Lourenco

## ► To cite this version:

Natália Galoro Leite, Matias Bermann, Shogo Tsuruta, Ignacy Misztal, Daniela Lourenco. Marker effect p-values for single-step GWAS with the algorithm for proven and young in large genotyped populations. *Genetics Selection Evolution*, 2024, 56 (1), pp.59. 10.1186/s12711-024-00925-3. hal-04677274

**HAL Id: hal-04677274**

**<https://hal.science/hal-04677274v1>**

Submitted on 26 Aug 2024

**HAL** is a multi-disciplinary open access archive for the deposit and dissemination of scientific research documents, whether they are published or not. The documents may come from teaching and research institutions in France or abroad, or from public or private research centers.

L'archive ouverte pluridisciplinaire **HAL**, est destinée au dépôt et à la diffusion de documents scientifiques de niveau recherche, publiés ou non, émanant des établissements d'enseignement et de recherche français ou étrangers, des laboratoires publics ou privés.

RESEARCH ARTICLE

Open Access



# Marker effect p-values for single-step GWAS with the algorithm for proven and young in large genotyped populations

Natália Galoro Leite<sup>1\*</sup> , Matias Bermann<sup>1</sup>, Shogo Tsuruta<sup>1</sup>, Ignacy Misztal<sup>1</sup> and Daniela Lourenco<sup>1</sup>

## Abstract

**Background** Single-nucleotide polymorphism (SNP) effects can be backsolved from ssGBLUP genomic estimated breeding values (GEBV) and used for genome-wide association studies (ssGWAS). However, obtaining p-values for those SNP effects relies on the inversion of dense matrices, which poses computational limitations in large genotyped populations. In this study, we present a method to approximate SNP p-values for ssGWAS with many genotyped animals. This method relies on the combination of a sparse approximation of the inverse of the genomic relationship matrix ( $\mathbf{G}_{APY}^{-1}$ ) built with the algorithm for proven and young (APY) and an approximation of the prediction error variance of SNP effects which does not require the inversion of the left-hand side (LHS) of the mixed model equations. To test the proposed p-value computing method, we used a reduced genotyped population of 50K genotyped animals and compared the approximated SNP p-values with benchmark p-values obtained with the direct inverse of LHS built with an exact genomic relationship matrix ( $\mathbf{G}^{-1}$ ). Then, we applied the proposed approximation method to obtain SNP p-values for a larger genotyped population composed of 450K genotyped animals.

**Results** The same genomic regions on chromosomes 7 and 20 were identified across all p-value computing methods when using 50K genotyped animals. In terms of computational requirements, obtaining p-values with the proposed approximation reduced the wall-clock time by 38 times and the memory requirement by ten times compared to using the exact inversion of the LHS. When the approximation was applied to a population of 450K genotyped animals, two new significant regions on chromosomes 6 and 14 were uncovered, indicating an increase in GWAS detection power when including more genotypes in the analyses. The process of obtaining p-values with the approximation and 450K genotyped individuals took 24.5 wall-clock hours and 87.66GB of memory, which is expected to increase linearly with the addition of noncore genotyped individuals.

**Conclusions** With the proposed method, obtaining p-values for SNP effects in ssGWAS is computationally feasible in large genotyped populations. The computational cost of obtaining p-values in ssGWAS may no longer be a limitation in extensive populations with many genotyped animals.

## Background

The single-step genomic best linear unbiased prediction (ssGBLUP) has been successfully implemented in the routine genetic evaluation of several livestock species [1–3]. The vast adoption of ssGBLUP is associated with the straightforward and simultaneous evaluation of populations composed of genotyped and non-genotyped animals, the non-requirement of pseudo phenotypes,

\*Correspondence:

Natália Galoro Leite  
nataliabaraviera@gmail.com

<sup>1</sup> Department of Animal and Dairy Science, University of Georgia, Athens, GA 30602, USA



the decrease in biases attributed to double counting and genomic preselection, and reliable estimation of breeding values for complex genetic models [4].

Although ssGBLUP is a breeding value-based method that provides genomic estimated breeding values (GEBVs), obtaining single-nucleotide polymorphism (SNP) effects from this method may also be valuable when investigating how genome segments are associated with important traits. When that is the case, SNP effects can be easily obtained from a linear transformation of GEBVs following formulas presented by VanRaden [5], Strandén and Garrick [6], and Wang et al. [7]. Besides SNP effects, the proportion of genetic variance explained by single SNPs or by SNP windows can help identify important regions of the genome in single-step genome-wide association studies (ssGWAS) [8–10]. However, this procedure does not consider the uncertainty of the SNP effect estimation, making it more difficult to replicate findings from ssGWAS [9, 10]. To overcome this problem, Aguilar et al. [11] presented formulas for obtaining frequentist p-values for ssGWAS as an extension of the ideas previously presented by Gualdrón Duarte et al. [12], Bernal Rubio et al. [13], and Lu et al. [14] in the ssGBLUP context. The authors also showed that p-values could be successfully obtained within a reasonable computational time for a large Angus population accounting for roughly 1M phenotyped individuals, 1500 genotyped sires, and about 1.8M animals in the pedigree.

The formulas presented by Aguilar et al. [11] require obtaining the prediction error variance of the SNP effects ( $\text{var}(\hat{a}_i)$ ) which relies on obtaining the breeding value prediction error (co)variance for genotyped animals ( $\mathbf{C}^{u_2c}$ ) through the inversion of the left-hand side (LHS) of the mixed model equations. The inversion of such a matrix becomes challenging as the number of traits and genotyped animals increases. With genomic information, the LHS is associated with a very dense block represented by the inverse of the genomic relationship matrix ( $\mathbf{G}^{-1}$ ), which is hard to obtain directly for more than 100K genotyped animals [4]. One approach to deal with the computation limits with large genotyped populations is to use a sparse approximation of  $\mathbf{G}^{-1}$  created by the algorithm for proven and young (APY) [15]. In APY, the genotyped individuals are split into two sets. The set of genotyped animals representing all genomic variation is called “core” (non-redundant information); the remaining animals are “noncore” (redundant information). Then, the GEBVs of noncore animals are conditioned on the GEBVs of core animals, making  $\mathbf{G}^{-1}$  very sparse. Apart from increasing the sparseness of  $\mathbf{G}^{-1}$ , Bermann et al. [16] showed that, with APY, obtaining  $\text{var}(\hat{a}_i)$  can be reduced to components only associated with the prediction error covariance of GEBVs for the core set ( $\mathbf{C}^{u_2c}$ ), drastically reducing the dimensionality of

matrices involved in calculations to obtain  $\text{var}(\hat{a}_i)$ . However, in the formulas shown by Bermann et al. [16], obtaining  $\mathbf{C}^{u_2c}$  still requires a direct inversion of the LHS with all genotyped animals. Even though  $\mathbf{G}^{-1}$  is sparser with APY, components in the LHS of single-step equations such as the inverse of the pedigree relationship matrix for genotyped animals ( $\mathbf{A}_{22}^{-1}$ ) are still dense, thus implying that computation limits for the inversion of LHS might still exist.

One way to overcome this problem is to obtain an approximated prediction error (co)variance of GEBVs for the APY core set ( $\mathbf{C}^{u_2c}$ ) that does not require the inversion of the LHS. For that, an extension of the algorithm proposed by Misztal and Wiggans [17] that accounts for genomic information with APY was presented by Bermann et al. [18]. In this algorithm, Bermann et al. [18] showed that  $\mathbf{C}^{u_2c}$  can be obtained with a block-sparse inversion of  $\mathbf{G}^{-1}$  with APY ( $\mathbf{G}_{\text{APY}}^{-1}$ ) plus a diagonal matrix of contributions from phenotypes and pedigree relationships. Empirical results shown by the authors demonstrate that  $\mathbf{C}^{u_2c}$  is obtained in a few minutes for an Angus population with about 300K genotyped animals. Moreover, they showed that, although computation complexity increases cubically with the number of core animals, that remains linear for the noncore set. Thus, combining APY and  $\mathbf{C}^{u_2c}$  should enable the approximation of p-values for ssGWAS for large genotyped populations within a feasible amount of time and computational resources. Therefore, this study presents a method to approximate SNP p-values for large genotyped populations based on APY. The performance of the proposed method was tested against the regular way to compute p-values using the exact inverse of LHS with  $\mathbf{G}^{-1}$  or  $\mathbf{G}_{\text{APY}}^{-1}$  with 50K genotyped animals. Then, the final test involved applying the proposed approximation method to a dataset with 450K genotyped animals.

## Methods

### Theory

In ssGBLUP, SNP effects can be obtained from backsolving GEBV using a linear transformation [5–7]:

$$\hat{\mathbf{a}} = (1 - \beta) \mathbf{b} \frac{\sigma_u^2}{\sigma_a^2} \mathbf{Z}' \mathbf{G}^{-1} \hat{\mathbf{u}}, \tag{1}$$

where  $\hat{\mathbf{a}}$  is the vector of SNP effects,  $\beta$  is the blending parameter (5%) to avoid singularity problems in  $\mathbf{G}$  [5];  $\mathbf{b}$  is a tuning parameter [19],  $\sigma_u^2$  is the genetic variance,  $\sigma_a^2$  is SNP variance,  $\mathbf{Z}$  is a matrix of SNP content centered by two times the allele frequency ( $p$ ),  $\hat{\mathbf{u}}$  is the vector of GEBVs, and  $\mathbf{G}^{-1}$  is the inverse of the genomic relationship matrix, with  $\mathbf{G}$  constructed as the type I of VanRaden [5]:

$$\mathbf{G} = (1 - \beta) \left( \mathbf{1}\mathbf{1}'\alpha + b \frac{\mathbf{Z}\mathbf{Z}'}{2 \sum p_i (1 - p_i)} \right) + \beta \mathbf{A}_{22}, \tag{2}$$

where  $\alpha$  and  $b$  are tuning parameters to assure the compatibility between  $\mathbf{G}$  and  $\mathbf{A}_{22}$  [19], and other elements were defined above.

Once SNP effects ( $\hat{\mathbf{a}}$ ) are estimated, the p-value for the  $i$ th SNP can be obtained as shown by Aguilar et al. [11]:

$$p - \text{value}_i = 2 \left( 1 - \Phi \left( \left| \frac{\hat{a}_i}{\text{sd}(\hat{a}_i)} \right| \right) \right), \tag{3}$$

where  $\text{sd}(\hat{a}_i)$  is the square root of the variance of the  $i$ th SNP effect estimate obtained as [12]:

$$\text{var}(\hat{a}_i) = \frac{1}{2 \sum p_i (1 - p_i)} (1 - \beta) \mathbf{b}\mathbf{z}'_i \mathbf{G}^{-1} (\mathbf{G}\sigma_u^2 - \mathbf{C}^{u_2 u_2}) \mathbf{G}^{-1} \mathbf{z}_i (1 - \beta) b \frac{1}{2 \sum p_i (1 - p_i)}, \tag{4}$$

with  $\mathbf{C}^{u_2 u_2}$  referring to the matrix of GEBV prediction error (co)variance for genotyped animals, and other parameters are defined above. The computation of  $\text{var}(\hat{a}_i)$  is restrained by the costs associated with obtaining  $\mathbf{G}^{-1}$  and  $\mathbf{C}^{u_2 u_2}$ . Those components result from the inversion of dense matrices of high dimension, and obtaining them becomes unfeasible with large genotyped populations [11, 20].

The computational limitations of obtaining  $\mathbf{G}^{-1}$  can be overcome by replacing this matrix with a sparse approximation built with APY [15]. With APY, a small set of genotyped animals (core) is chosen, and the relationship of the remaining animals (noncore) is obtained by recursions on the core set with linear computing cost. The inverse of the genomic relationship matrix with APY is constructed as follows:

$$\mathbf{G}_{\text{APY}}^{-1} = \begin{bmatrix} \mathbf{G}_{\text{cc}}^{-1} & \mathbf{0} \\ \mathbf{0} & \mathbf{0} \end{bmatrix} + \begin{bmatrix} -\mathbf{G}_{\text{cc}}^{-1} \mathbf{G}_{\text{cn}} \\ \mathbf{I} \end{bmatrix} \mathbf{M}_{\text{nn}}^{-1} \begin{bmatrix} -\mathbf{G}_{\text{nc}} \mathbf{G}_{\text{cc}}^{-1} & \mathbf{I} \end{bmatrix} = \begin{bmatrix} \mathbf{G}_{\text{cc}}^{-1} + \mathbf{G}_{\text{cc}}^{-1} \mathbf{G}_{\text{cn}} \mathbf{M}_{\text{nn}}^{-1} \mathbf{G}_{\text{nc}} \mathbf{G}_{\text{cc}}^{-1} & -\mathbf{G}_{\text{cc}}^{-1} \mathbf{G}_{\text{cn}} \mathbf{M}_{\text{nn}}^{-1} \\ -\mathbf{M}_{\text{nn}}^{-1} \mathbf{G}_{\text{nc}} \mathbf{G}_{\text{cc}}^{-1} & \mathbf{M}_{\text{nn}}^{-1} \end{bmatrix} = \begin{bmatrix} \mathbf{G}^{\text{cc}} & \mathbf{G}^{\text{cn}} \\ \mathbf{G}^{\text{nc}} & \mathbf{M}_{\text{nn}}^{-1} \end{bmatrix}, \tag{5}$$

where  $\mathbf{G}_{\text{cc}}^{-1}$  and  $\mathbf{M}_{\text{nn}}^{-1}$  are the inverses of the full genomic relationship matrix for core and diagonal for noncore animals, respectively, and  $\mathbf{G}_{\text{cn}}$  is the genomic relationship matrix between core and noncore animals. The elements of the matrix  $\mathbf{M}_{\text{nn}}^{-1}$  are obtained as:

$$\mathbf{m}_{\text{nn},j} = \text{diag} \left\{ \mathbf{g}_{jj} - \mathbf{g}'_{jc} \mathbf{G}_{\text{cc}}^{-1} \mathbf{g}_{cj} \right\}, \tag{6}$$

where  $\mathbf{g}_{jj}$  is the diagonal element of  $\mathbf{G}_{\text{nn}}$  for the  $j$ th animal, and  $\mathbf{g}_{jc}$  is the relationship between the  $j$ th noncore animal with core animals. With APY, the need to invert a dense and high dimensional  $\mathbf{G}$  is reduced to only inverting the genomic relationship matrix for core animals ( $\mathbf{G}_{\text{cc}}$ ) [Eq. (5)], which for most livestock species or breeds contains less than 15K animals [21, 22].

Beyond the reductions in computing costs of obtaining  $\mathbf{G}^{-1}$ , Bermann et al. [16] showed that, with APY, estimating the  $\text{var}(\hat{a}_i)$  as in Eq (4) is reduced to components only associated with the core animals:

$$\text{var}(\hat{a}_i) = \frac{1}{2 \sum p_i (1 - p_i)} (1 - \alpha) \mathbf{b}\mathbf{z}'_{cj} \mathbf{G}_{\text{CC}}^{-1} (\mathbf{G}_{\text{CC}} \sigma_u^2 - \mathbf{C}^{u_2 c u_2 c}) \mathbf{G}_{\text{CC}}^{-1} \mathbf{z}_{cj} (1 - \alpha) b \frac{1}{2 \sum p_i (1 - p_i)}, \tag{7}$$

where  $\mathbf{z}_{cj}$  is the  $j$ th column of the  $\mathbf{Z}$  matrix for core animals, and  $\mathbf{C}^{u_2 c u_2 c}$  is the prediction error (co)variance matrix of GEBVs for core animals, and other elements are as defined before. However, obtaining  $\mathbf{C}^{u_2 c u_2 c}$ , still depends on the inversion of a high dimension LHS, which might yet limit computations as model complexity and the number of genotyped animals increase. To overcome this limitation, an approximation of the prediction error (co)variance matrix of GEBVs for core animals ( $\mathbf{C}^{u_2 c u_2 c \text{approx}}$ ) can be obtained as follows [18]:

$$\mathbf{C}^{u_2 c u_2 c \text{approx}} = \left( \mathbf{D}_c + \lambda \mathbf{G}^{\text{cc}} - \lambda \mathbf{G}^{\text{cn}} \left( \lambda \mathbf{M}_{\text{nn}}^{-1} + \mathbf{D}_n \right)^{-1} \lambda \mathbf{G}^{\text{nc}} \right)^{-1}, \tag{8}$$

where  $\lambda = \frac{\sigma_e^2}{\sigma_u^2}$ ,  $\sigma_e^2$  is the residual variance, and  $\mathbf{D}_c$  and  $\mathbf{D}_n$  are the blocks for core and noncore animals from the diagonal matrix  $\mathbf{D}$  constructed as [17, 23]:

$$\mathbf{D} \approx \mathbf{W}' (\mathbf{I} - \mathbf{X}(\mathbf{X}'\mathbf{X})^{-1} \mathbf{X}') \mathbf{W}, \tag{9}$$

where  $\mathbf{W}$  and  $\mathbf{X}$  are incidence matrices for animal and fixed effects. Therefore, when combining APY and  $\mathbf{C}^{u_2 c u_2 c \text{approx}}$  the  $\text{var}(\hat{a}_i)$  can be approximated as:

$$\text{var}(\hat{a}_i) \approx \frac{1}{2 \sum p_i (1 - p_i)} (1 - \alpha) \mathbf{b}\mathbf{z}'_{cj} \mathbf{G}_{\text{CC}}^{-1} (\mathbf{G}_{\text{CC}} \sigma_u^2 - \mathbf{C}^{u_2 c u_2 c \text{approx}}) \mathbf{G}_{\text{CC}}^{-1} \mathbf{z}_{cj} (1 - \alpha) b \frac{1}{2 \sum p_i (1 - p_i)}, \tag{10}$$

where all parameters were defined above. Equation (10) implies that when APY and  $\mathbf{C}^{\mathbf{u}_2\mathbf{c}\mathbf{u}_2\mathbf{c}_{approx}}$  are combined, SNP p-values can be calculated with matrices only associated with core animals and without the requirement of inverting the LHS, thus potentially lifting the current computational limitations for large genotyped populations.

Therefore, the proposed method to approximate p-values for SNP involves the following steps:

1. Save  $\mathbf{G}_{APY}^{-1}$  and components of  $\mathbf{A}_{22}^{-1}$  [24] in disk (PREGSF90 from BLUPF90 software suite; Misztal et al. [25]);
2. Obtain GEBVs based on APY by reading the saved matrices (BLUP90IOD3 from BLUPF90 software suite);
3. Compute  $\mathbf{C}^{\mathbf{u}_2\mathbf{c}\mathbf{u}_2\mathbf{c}_{approx}}$  using block sparse inversion as in Bermann et al. (2022b) (ACCF90GS2 from BLUPF90 software suite);
4. Use  $\mathbf{C}^{\mathbf{u}_2\mathbf{c}\mathbf{u}_2\mathbf{c}_{approx}}$  and  $\mathbf{G}_{cc}^{-1}$  from  $\mathbf{G}_{APY}^{-1}$  to compute  $\text{var}(\hat{\mathbf{a}}_i)$  as in Eq. (10) (POSTGSF90 from BLUPF90 software suite);
5. Backsolve SNP effects from GEBVs obtained in step 2 as in Eq. (1) with  $\mathbf{G}_{APY}^{-1}$ ; compute SNP p-values, as in Eq. (3) by using the square root of  $\text{var}(\hat{\mathbf{a}}_i)$  obtained in step 4 (POSTGSF90 from BLUPF90 software suite).

### Dataset

The American Angus Association (Saint Joseph, MO) provided the dataset to test the proposed method to approximate p-values for SNP. A total of 844,726 animals born from 2012 to 2017 were scored for post-weaning gain (PWG). Phenotyped animals were produced by 93,161 sires and 812,292 cows and were distributed into 64,889 contemporary groups. Genomic information on 39,744 SNP (after quality control) was available for 450,673 animals born from 2012 to 2018. Of the genotyped animals, 217,434 were also phenotyped, whereas the remaining animals only contributed with genotypes and pedigree. Pedigree information was available for all phenotyped and genotyped animals up to 3 generations of relationships, summing up 1,837,789 records.

### Reduced dataset

In this study we aimed to compare different p-value computing methods, where p-values obtained from a direct inversion of the LHS were used as benchmark (see Statistical analyses for more details). Due to the computational limitations of inverting the LHS, a reduced genomic subset of 50K randomly selected genotyped animals was created. As the subset of 50K genotyped animals were

selected randomly, the sampling process was repeated three times, thus three reduced genotype subsets were created. Phenotypic information was kept complete for all replicates. However, the number of animals in the pedigree varied slightly (from 1,576,112 to 1,576,738). This small variation is due to the creation of the pedigree in a way that it traces back three generations for phenotyped and genotyped animals in the dataset, and for the reduced datasets, genotyped animals varied because of sampling.

### Statistical model

A single-trait animal model was used for the estimation of PWG GEBVs as follows:

$$\mathbf{y} = \mathbf{X}\boldsymbol{\beta} + \mathbf{W}\mathbf{u} + \mathbf{e}, \quad (11)$$

where  $\mathbf{y}$  is the vector of PWG phenotypes;  $\boldsymbol{\beta}$  is the vector containing the fixed effect of contemporary groups;  $\mathbf{u}$  is the vector of random additive genetic effects;  $\mathbf{e}$  is the vector of random residuals; and  $\mathbf{X}$ , and  $\mathbf{W}$  are incidence matrices for the effects contained in  $\boldsymbol{\beta}$  and  $\mathbf{u}$ , respectively. Random effects were distributed as  $\mathbf{e} \sim N(\mathbf{0}, \mathbf{I}\sigma_e^2)$  and  $\mathbf{u} \sim N(\mathbf{0}, \mathbf{H}\sigma_u^2)$ , where  $\mathbf{I}$  is an identity matrix, and  $\mathbf{H}$  is the realized relationship matrix for genotyped and non-genotyped animals in ssGBLUP, with inverse constructed as shown by Aguilar et al. [26]:

$$\mathbf{H}^{-1} = \mathbf{A}^{-1} + \begin{bmatrix} \mathbf{0} & \mathbf{0} \\ \mathbf{0} & \mathbf{T}^{-1} - \mathbf{A}_{22}^{-1} \end{bmatrix}, \quad (12)$$

where  $\mathbf{A}^{-1}$  is the inverse of the pedigree relationship matrix and  $\mathbf{T}^{-1}$  is equal to  $\mathbf{G}_{APY}^{-1}$  [Eq. (5)] for genetic analyses with APY, and equal to  $\mathbf{G}^{-1}$  [Eq. (2)] otherwise. The  $\mathbf{A}_{22}^{-1}$  was built as defined before.

### Statistical analyses

#### Comparison between p-value computing methods in a small genotyped population

In this set of analyses, we aimed to compare exact p-values obtained with a regular  $\mathbf{G}^{-1}$  and  $\mathbf{C}^{\mathbf{u}_2\mathbf{u}_2}$  (Exact\_Ginv) as a benchmark [Eqs. (3) and (4)], with p-values with  $\mathbf{G}_{APY}^{-1}$  and exact  $\mathbf{C}^{\mathbf{u}_2\mathbf{c}\mathbf{u}_2\mathbf{c}}$  (Exact\_GinvAPY) [Eqs. (3) and (7)], and p-values obtained with  $\mathbf{G}_{APY}^{-1}$  and  $\mathbf{C}^{\mathbf{u}_2\mathbf{c}\mathbf{u}_2\mathbf{c}_{approx}}$  (Approx\_GinvAPY) [Eqs. (3) and (10)]. Because the p-values from Exact\_Ginv and Exact\_GinvAPY require obtaining the inverses of the genomic relationship matrix and of the LHS, a reduced subset of 50K was used to ensure computation feasibility and fair comparisons.

For methods involving APY (i.e., Exact\_GinvAPY and Approx\_GinvAPY), the APY core was composed of 13,030 genotypes, which corresponded to the number of eigenvalues explaining 98% of the genetic variance in

**G.** This was obtained applying the singular value decomposition of  $\mathbf{Z}$  composed of all genotypes available (i.e., 450 K) [22]. The selection of core animals was made at random. This decision was supported by previous studies showing the performance of random core selection in comparison to alternative selection strategies [3, 27, 28]. Moreover, as the genotyped set was reduced to 50K for this set of analyses, that also reduced opportunities to high contrasts for the core-noncore compositions (i.e., core composed of sires with high accuracies or with large number of genotyped progeny).

After all analyses performed, p-value computing methods were compared based on the Pearson correlation of computed p-values, SNP effects,  $\text{var}(\hat{a}_i)$ , in addition to the inspection of Manhattan and QQ plot results. Wall-clock time and Resident Set Size (RSS) memory requirements were also recorded.

**Application of Approx\_GinvAPY in a large genotyped population**

In the second set of analyses, we aimed to calculate p-values with  $\mathbf{G}_{\text{APY}}^{-1}$  and  $\mathbf{C}^{\text{u}_2\text{c}\text{u}_2\text{c}_{\text{approx}}}$  with the full set of 450K genotyped animals (Approx\_GinvAPY450K). Note that, Approx\_GinvAPY and Approx\_GinvAPY450K comprised the same p-value computing method, the only difference is the size of the genotype set (50K vs. 450K, respectively). For straightforward interpretations, within the same replicate, the core sets in Approx\_GinvAPY450K were composed of the same set of animals as with the analyses with the reduced dataset. For example, within each replicate, the core set in Exact\_Ginv, Approx\_GinvAPY, and Approx\_GinvAPY450K consisted of the same genotyped animals.

To evaluate the robustness of the proposed p-value computing method regarding core composition, we ran an extra scenario where the APY core of Approx\_GinvAPY450K was composed of genotyped animals with the highest estimated breeding value (EBV) accuracies in the population (Approx\_GinvAPY450K\_high-acc). EBV accuracies were obtained in a previous step without including genomic information, which means their merit was mainly based on progeny contributions. The core dimension was kept constant at 13,030 genotypes.

Elapsed wall-clock time and RSS memory requirements were recorded. The inspection of Manhattan and QQ plots results were used to evaluate the soundness of the approximation applied to the full genotype set. A summary of the information available for all analyses with reduced or full genotype sets is displayed in Table 1.

For all GWAS analyses performed in this study, a significance level of 5% adjusted by multiple testing via Bonferroni correction was used as a SNP rejection

**Table 1** Number of records per source of information for all p-value computing methods

Method <sup>a</sup>	Genotypes	Core	Pedigree	Phenotypes
Exact_Ginv	50,000	13,030	1,576,738 <sup>b</sup>	844,726
Exact_GinvAPY	50,000	13,030	1,576,738 <sup>b</sup>	844,726
Approx_GinvAPY	50,000	13,030	1,576,738 <sup>b</sup>	844,726
Approx_GinvAPY450K	450,673	13,030	1,837,789	844,726

<sup>a</sup> SNP p-values obtained from a data set of 50K genotyped with  $\mathbf{G}^{-1}$  and  $\mathbf{C}^{\text{u}_2\text{u}_2}$  (Exact\_Ginv),  $\mathbf{G}_{\text{APY}}^{-1}$  and  $\mathbf{C}^{\text{u}_2\text{c}\text{u}_2\text{c}}$ (Exact\_GinvAPY), and  $\mathbf{G}_{\text{APY}}^{-1}$  and  $\mathbf{C}^{\text{u}_2\text{c}\text{u}_2\text{c}_{\text{approx}}}$  (Approx\_GinvAPY). Approx\_GinvAPY450K refers to the Approx\_GinvAPY method applied to a genotyped population of 450K animals

<sup>b</sup> Because pedigree traced back three generations of relationships from phenotyped and genotyped animals, the number of animals in the pedigree slightly varied from 1,576,112 to 1,576,738 between replicates

threshold, i.e.,  $-\log(0.05/m)$ ; where  $m$  (39,744) is the number of markers in the SNP panel. As the SNP panel density was kept constant throughout this study, this implies a fixed rejection threshold for all sets of analyses and comparisons. Moreover, all analyses were performed with software from the BLUPF90 software suite [25] on an Intel(R) Xeon(R) CPU E5-2650 v4 @ 2.20 GHz server with 24 threads. New implementations for obtaining p-values with  $\mathbf{G}_{\text{APY}}^{-1}$  and  $\mathbf{C}^{\text{u}_2\text{c}\text{u}_2\text{c}_{\text{approx}}}$  were available in modified versions of BLUP90IOD3 and ACCF90GS2 [29].

**Results and discussion**

Using ssGWAS for association studies in farm animal populations increases the detection power because it considers phenotypic information from non-genotyped individuals, allows for complex models involving multiple traits and environmental and genetic correlated effects, and does not rely on pseudo phenotypes [10, 30, 31]. However, computing SNP p-values from ssGWAS still depends on the inversion of the LHS and should become prohibited with increasing data dimensionality. In this study, we approach the challenge of computing p-value in populations with an increasing number of genotyped individuals with APY. For that, we compared three methods to calculate p-values, which consisted of obtaining p-values with (1) a regular  $\mathbf{G}^{-1}$  and  $\mathbf{C}^{\text{u}_2\text{u}_2}$  (Exact\_Ginv), (2) with  $\mathbf{G}_{\text{APY}}^{-1}$  and exact  $\mathbf{C}^{\text{u}_2\text{c}\text{u}_2\text{c}}$  (Exact\_GinvAPY), and (3) an efficient method combining  $\mathbf{G}_{\text{APY}}^{-1}$  and  $\mathbf{C}^{\text{u}_2\text{c}\text{u}_2\text{c}_{\text{approx}}}$  (Approx\_GinvAPY). We later evaluated the performance of the Approx\_GinvAPY method when applied to a large genotyped population comprised of around 450K individuals with a random core composition (Approx\_GinvAPY450K) and with a core composed of genotyped animals with the highest EBV accuracies in the population (Approx\_GinvAPY450K\_high-acc).

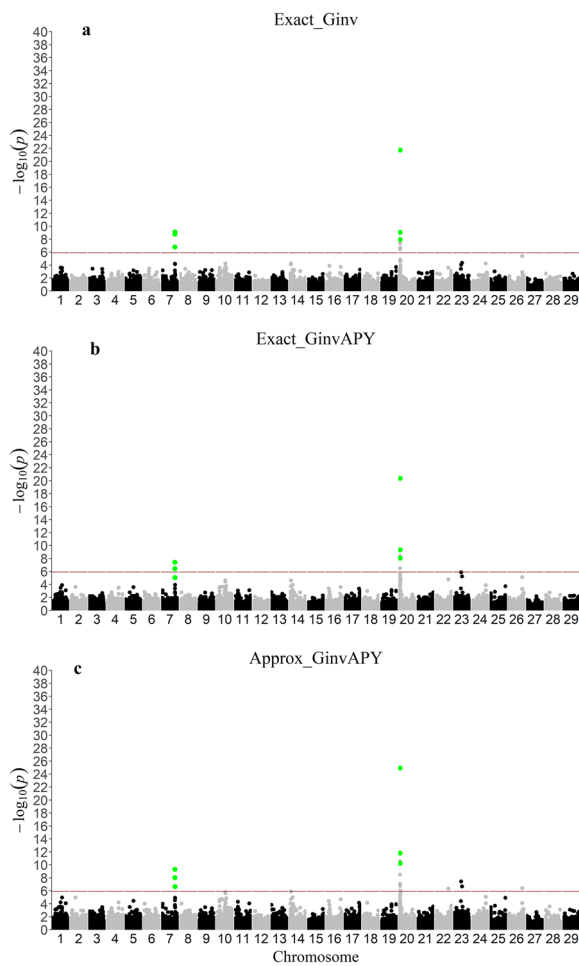


**Fig. 1** Manhattan plots for all p-value computing methods with a reduced data set in replicate 1. Single-step genome-wide association study for post-weaning weight with p-values obtained from a data set of 50K genotyped animals with (A)  $G^{-1}$  and  $C^{u_2u_2}$  (Exact\_Ginv), (B)  $G_{APY}^{-1}$  and  $C^{u_2c u_2c}$  (Exact\_GinvAPY), and (C)  $G_{APY}^{-1}$  and  $C^{u_2c u_2c approx}$  (Approx\_GinvAPY) in replicate 1; SNPs highlighted in green represent the three most significant SNP in the two peaks found with Exact\_Ginv (benchmark)

**Comparison between p-value computing methods in a small genotyped population**

Manhattan and QQ plots for all investigated p-value computing methods in replicate 1 are shown in Figs. 1 and 2, respectively. Manhattan and QQ plots for replicates 2 and 3 are provided in Additional file 1: Figures S1, S2, S3, and S4. Across all methods and replicates, two significant peaks were identified on chromosomes 7 and 20 for PWG. For the peak on chromosome 7, the same top three SNPs were identified across all methods. However, for the peak on chromosome 20 only the first top SNP was consistent across p-value computing methods; the second and third top SNP slightly varied across

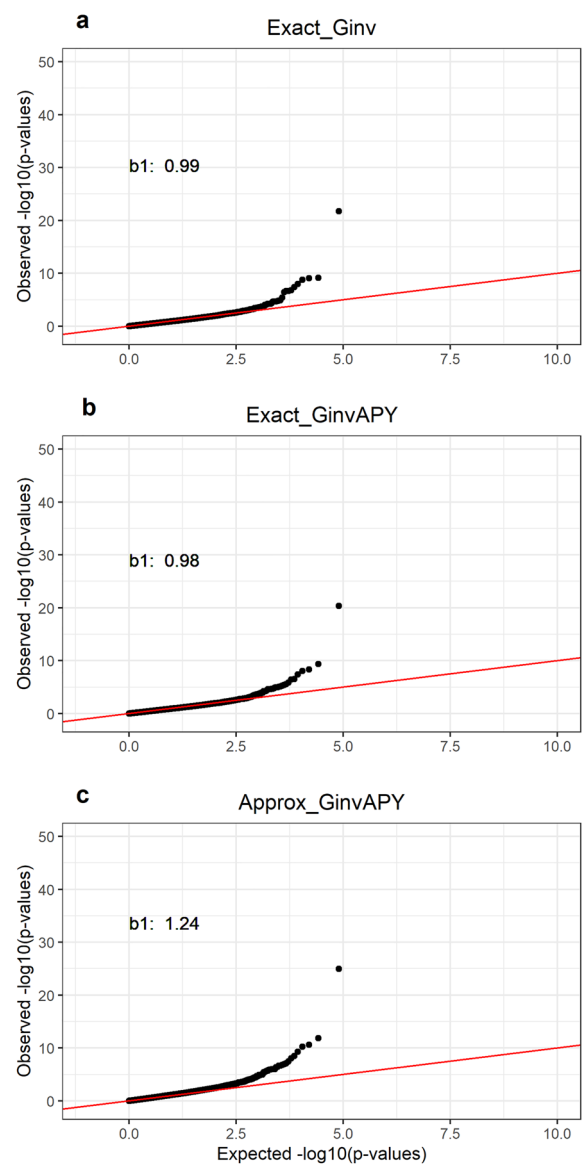


**Fig. 2** QQ plots for all p-value computing methods with a reduced data set in replicate 1. QQ plots for p-values obtained from a data set of 50K genotyped animals with A  $G^{-1}$  and  $C^{u_2u_2}$  (Exact\_Ginv), B  $G_{APY}^{-1}$  and  $C^{u_2c u_2c}$  (Exact\_GinvAPY), and C  $G_{APY}^{-1}$  and  $C^{u_2c u_2c approx}$  (Approx\_GinvAPY) in replicate 1

neighboring SNPs within a 2Mb window (Fig. 1, Additional file 1: Figures S1 and S2).

Despite the overall correct identification of the same SNPs with all p-values computing methods, the Approx\_GinvAPY method resulted in a higher deviation of p-values from the null hypothesis in comparison to results from Exact\_Ginv (Fig. 2, Additional file 1: Figures S3 and S4). Across replicates, the slope of the QQ plot for Exact\_Ginv and Exact\_GinvAPY was nearly constant at 0.99 ( $0.99 \pm 0.01$  and  $0.99 \pm 0.02$ , respectively), while the

**Table 2** Person correlation between all (above diagonal) and significant<sup>a</sup> (below diagonal) p-values, SNP effects, and variance of estimated SNP effects across methods

Method <sup>b</sup>	p-value		
	Exact_Ginv	Exact_GinvAPY	Approx_GinvAPY
Exact_Ginv		0.82 ± 0.02	0.82 ± 0.02
Exact_GinvAPY	0.91 ± 0.02		1.00 ± 0.00
Approx_GinvAPY	0.91 ± 0.02	1.00 ± 0.00	
var( $\hat{a}_i$ )	p-value		
	Exact_Ginv	Exact_GinvAPY	Approx_GinvAPY
Exact_Ginv		0.91 ± 0.00	0.92 ± 0.00
Exact_GinvAPY			0.99 ± 0.00
Approx_GinvAPY			
$\hat{a}_i$	p-value		
	Exact_Ginv	Exact_GinvAPY	Approx_GinvAPY
Exact_Ginv		0.88 ± 0.01	0.88 ± 0.01
Exact_GinvAPY			1.00 ± 0.00
Approx_GinvAPY			

<sup>a</sup> Significant SNPs were defined based on Exact\_Ginv across replicates. <sup>b</sup> Methods refer to SNP p-values obtained from a data set of 50K genotyped animals with  $\mathbf{G}^{-1}$  and  $\mathbf{C}^{u_2 u_2}$  (Exact\_Ginv),  $\mathbf{G}_{APY}^{-1}$  and  $\mathbf{C}^{u_2 c u_2 c}$  (Exact\_GinvAPY), and  $\mathbf{G}_{APY}^{-1}$  and  $\mathbf{C}^{u_2 c u_2 c approx}$  (Approx\_GinvAPY)

slope of the QQ plot for Approx\_GinvAPY increased to  $1.25 \pm 0.03$ , indicating an overestimation of  $-\log_{10}(p\text{-values})$  with our proposed method. In practice, this overestimation can be corrected by the genomic control method proposed by Devlin and Roeder [32]

Correlations of p-values, SNP effects,  $\text{var}(\hat{a}_i)$  across p-value computing methods are displayed in Table 2. Between APY-based methods and Exact\_Ginv, correlations were, on average across replicates, constant at 0.82 for p-values, 0.88 for SNP effects, and ranged from 0.91 to 0.92 for  $\text{var}(\hat{a}_i)$ . When only significant p-values were considered, the correlation was increased to 0.91 (Table 2). In contrast, between APY-based methods, the correlation for all p-values, significant p-values, SNP effects, and  $\text{var}(\hat{a}_i)$ , and p-values approached unity (from 0.99 to 1.00) (Table 2). Those results demonstrate the goodness of the approximation of  $\mathbf{C}^{u_2 c u_2 c}$  ( $\mathbf{C}^{u_2 c u_2 c approx}$ ) (i.e., Exact\_GinvAPY vs. Approx\_GinvAPY), but also indicate an increase in noise mostly sourced from the use of APY (Exact\_Ginv vs. Exact\_GinvAPY and Approx\_GinvAPY). When approximations are used, errors can be accumulated, especially when multiple steps are involved. For example, for obtaining SNP effects with ssGBLUP, GEBVs are backsolved into SNP effects [Eq. (1)]. For APY-based methods, GEBVs have small changes compared to using

**Table 3** Elapsed wall-clock time and Resident Set Size (RSS) memory requirement for all p-values computation methods

Method <sup>a</sup>	Software	Elapsed time, h:min	SD	Peak of memory, GB	SD
Exact_Ginv	PREGSF90	1:01	0:27	107.28	0.00
	BLUPF90IOD3	93:13	21:20	159.66	0.88
	POSTGSF90	12:31	0:21	145.39	0.58
	Total/Max	106:46		159.66	
Exact_GinvAPY	PREGSF90	0:20	0:01	9.07	0.00
	BLUPF90IOD3	108:45	22:33	178.30	0.00
	POSTGSF90	1:53	0:39	44.83	0.00
	Total/Max	110:59		178.30	
Approx_GinvAPY	PREGSF90	0:39	0:16	9.07	0.00
	BLUPF90IOD3	0:54	0:21	4.53	0.00
	ACCF90GS2	0:04	0:02	9.07	0.00
	POSTGSF90	1:50	0:06	16.62	0.00
	Total/Max	2:50		16.62	

<sup>a</sup> SNP p-values obtained from a data set of 50K genotyped with  $\mathbf{G}^{-1}$  and  $\mathbf{C}^{u_2 u_2}$  (Exact\_Ginv),  $\mathbf{G}_{APY}^{-1}$  and  $\mathbf{C}^{u_2 c u_2 c}$  (Exact\_GinvAPY), and  $\mathbf{G}_{APY}^{-1}$  and  $\mathbf{C}^{u_2 c u_2 c approx}$  (Approx\_GinvAPY)

<sup>b</sup> Resident Set Size (RSS) memory. Values are displayed as average and standard deviations among three replicates

$\mathbf{G}^{-1}$  [33]. Then, the GEBVs are backsolved with a formula that also involves  $\mathbf{G}_{APY}^{-1}$ . Therefore, potential errors can be accumulated, especially for Approx\_GinvAPY, where approximation algorithms are involved. A result from this increase in noise with approximated methods can be demonstrated in Figs. 1, S1, and S2, where few SNPs on chromosomes 22, 23, 26, and 29 achieved significance level without a clear linkage disequilibrium trail with Approx\_GinvAPY [34].

When obtaining p-values with Approx\_GinvAPY estimation noise can be associated with two uncertainty measurements, the first being APY. The algorithm for proven and young is based on the theory that genomic information is limited, and that all genetic variation is contained in a set of independent chromosome segments within a population. Given that a core group of animals would contain those segments, the GEBVs of noncore animals in the population could be estimated from the GEBVs of core animals in addition to an error term  $\Phi_n$  ( $\mathbf{u}_n = \mathbf{G}_{nc} \mathbf{G}_{cc}^{-1} \mathbf{u}_c + \Phi_n$ ), which is expected to approach zero when the core size approaches the rank of  $\mathbf{G}$  [16, 35]. Note that, when p-values are backsolved with Eq. (1),  $\mathbf{G}^{-1}$  is replaced by  $\mathbf{G}_{APY}^{-1}$  and  $\hat{\mathbf{u}}$  is the vector of GEBVs obtained with  $\mathbf{G}_{APY}^{-1}$  composing the LHS. Therefore, those two components are affected by the approximation with APY. The second measurement of uncertainty comes from computing  $\mathbf{C}^{u_2 c u_2 c approx}$ . As shown by Misztal and

Wiggans [17], the off-diagonal elements are not considered during the absorption of environmental effects into the mixed model equations for constructing **D**. Thus, is expected that, with *Approx\_GinvAPY*, there is a slight increase in noise, especially when the core set and data are small.

The elapsed wall-clock time and RSS memory requirement across p-value computing methods are shown in Table 3. Despite ssGWAS results being similar among methods, computing times varied considerably. The average total elapsed wall-clock was 106.76h for *Exact\_Ginv*, 110.98h for *Exact\_GinvAPY*, and was reduced to 2.83h with *Approx\_GinvAPY* (Table 3). Therefore, compared to *Exact\_Ginv*, the run time with *Approx\_GinvAPY* was reduced by approximately 38 times. The RSS memory requirement also varied across p-value computing methods; its peak was 159.66GB, 178.30GB, and 16.62GB for *Exact\_Ginv*, *Exact\_GinvAPY*, and *Approx\_GinvAPY*, respectively. Compared to *Exact\_Ginv*, the peak RSS memory requirement for obtaining p-values with *Approx\_GinvAPY* was about tenfold smaller.

The most computationally demanding scenario was *Exact\_GinvAPY*, with the computation of p-values taking a total wall-clock time run of 110.98h and a peak of RSS memory requirement of 178.30GB. Even though APY increases the sparsity of  $G^{-1}$  by ignoring the relationships between noncore animals, it still requires the storage of intermediate matrices and vectors. Moreover, the computational advantage with APY comes mainly from the block implementation with the preconditioned conjugate gradient (PCG) method, as shown by Masuda et al. [36]. However, in *Exact\_GinvAPY*, the LHS is still explicitly inverted, which does not use the sparse properties of  $G_{APY}^{-1}$  [37]. Although *Exact\_GinvAPY* has a similar computing performance as *Exact\_Ginv*, results from this method are helpful in this study to illustrate the feasibility of accurately computing p-values with  $G_{APY}^{-1}$ .

**Application of *Approx\_GinvAPY* in a large genotyped population**

Manhattan and QQ plots for p-values obtained with *Approx\_GinvAPY450K* and *Approx\_GinvAPY450K\_high-acc* are displayed in Figs. 3 and 4, respectively. Across all replicates and scenarios, the two significant peaks on chromosomes 7 and 20 observed in the first set of analyses with *Exact\_Ginv* (benchmark) were also identified with *Approx\_GinvAPY450K* and *Approx\_GinvAPY450K\_high-acc* (Fig. 3). For the peak on chromosome 7, the same top three SNPs were identified with *Approx\_GinvAPY450K* and *Approx\_GinvAPY450K\_high-acc*, which were consistent with benchmark results with the reduced dataset (i.e., *Exact\_Ginv*). For the peak on chromosome 20, the first two top SNPs were

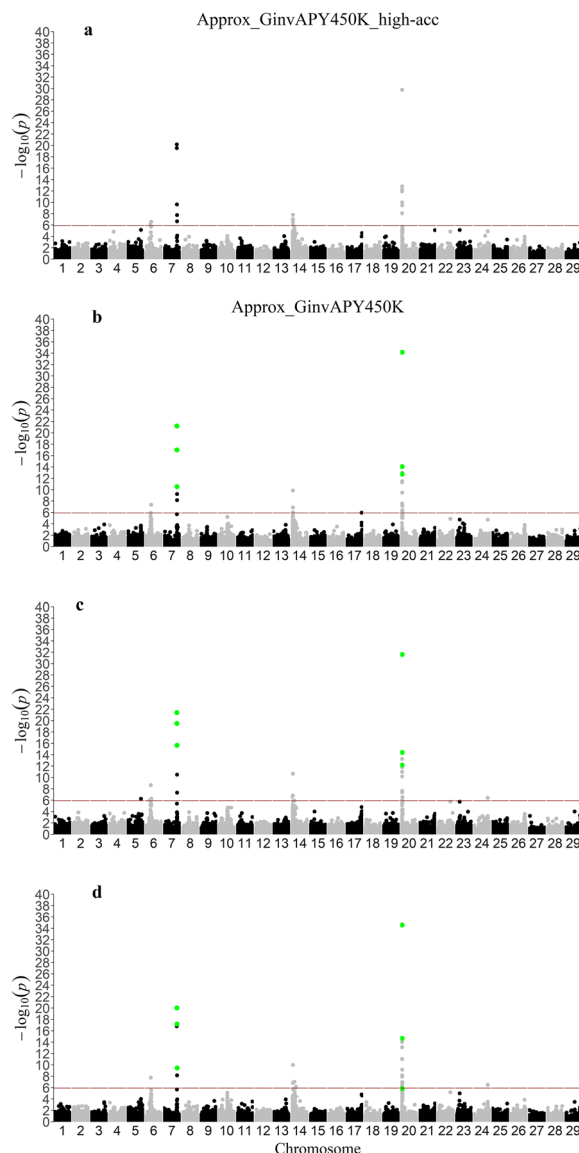


**Fig. 3** Single-step genome-wide association study for post-weaning weight using *Approx\_GinvAPY450K* and *Approx\_GinvAPY450K\_high-acc*. Single-step genome-wide association study for post-weaning weight using *Approx\_GinvAPY450K* in **A** replicate 1, **B** replicate 2, **C** replicate 3, and **D** using *Approx\_GinvAPY450K\_high-acc*; SNP highlighted in green represent the three most significant SNP in the two peaks found in with *Exact\_Ginv* with a reduced genotype dataset. *Approx\_GinvAPY450K* refers to the method where SNP p-values are obtained from a data set of 450K genotyped animals with  $G_{APY}^{-1}$  and  $C^{U_2C}U_2C_{approx}$  and where the APY core set if chosen at random; *Approx\_GinvAPY450K\_high-acc* refers to the *Approx\_GinvAPY450K* when the APY core is composed of animals with the highest EBV accuracy in the population

consistent across *Approx\_GinvAPY450K* and *Approx\_GinvAPY450K\_high-acc* while the third top SNP on chromosome 20 varied slightly across neighboring SNPs

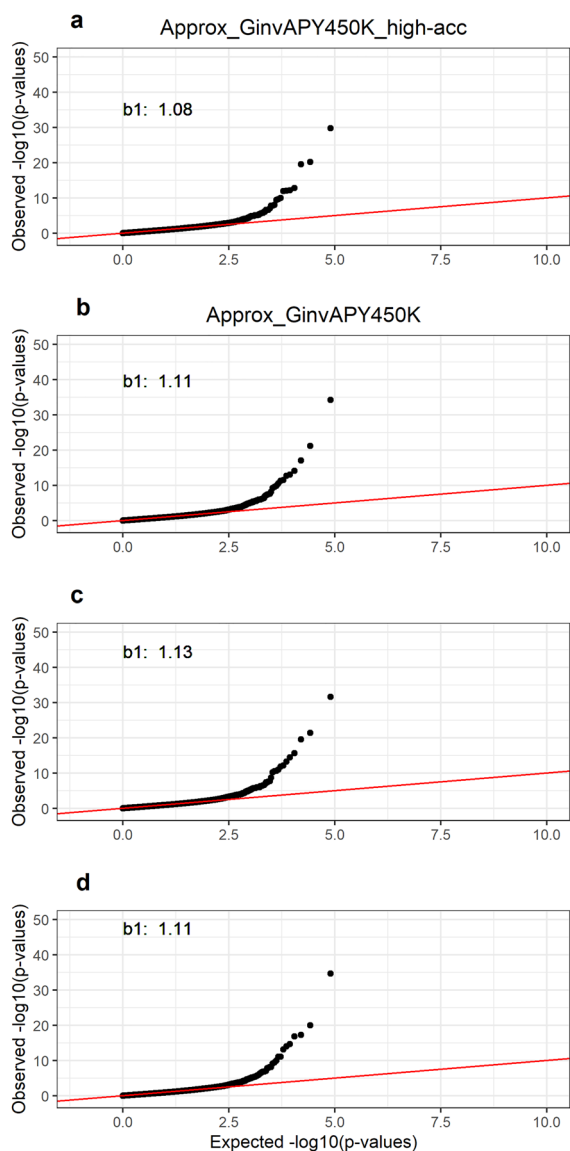


**Fig. 4** QQ plots for p-values obtained with Approx\_GinvAPY450K and Approx\_GinvAPY450K\_high-acc. QQ plots for p-values obtained with Approx\_GinvAPY450K in (A) replicate 1, (B) replicate 2, (C) replicate 3, and (D) with Approx\_GinvAPY450K\_high-acc. Approx\_GinvAPY450K refers to the method where SNP p-values are obtained from a data set of 450K genotyped animals with  $G_{APY}^{-1}$  and  $C^{u_2c u_2c_{approx}}$  and where the APY core set is chosen at random; Approx\_GinvAPY450K\_high-acc refers to the Approx\_GinvAPY450K when the APY core is composed of animals with the highest EBV accuracy in the population

within a 0.13Mb window (Fig. 3). Results from QQ plots were also very similar between Approx\_GinvAPY450K and Approx\_GinvAPY450K\_high-acc (Fig. 4). The slope of the QQ plot regression was 1.08 for Approx\_GinvAPY450K\_high-acc and  $1.12 \pm 0.01$  across Approx\_GinvAPY450K replicates, thus suggesting small influence of

core composition on the deviation of p-values from the null hypothesis. Despite the consistency of results with different core composition shown in this study, previous experience with a single breed population showed that, especially with datasets with a clear unbalance of phenotypic and genotypic information (i.e., phenotypic dataset with several generations of recording combined with only recent generations contributing with genotypes), the selection of APY core based on a random selection always resulted in the best solutions in comparison to benchmark results with the exact inversion of the LHS [38]. However, a more informed choice of core animals [3, 39] may be used without considerable changes of p-values for the significant peaks in well-structured, single-breed populations. Note that the optimum core composition strategy can change in multi-breed populations, especially when breed contributions are highly unbalanced [21].

Enlarging the genotype set also uncovered two new peaks on chromosomes 6 and 14 that were not observed with the reduced dataset (Fig. 3). The new peaks had clear linkage disequilibrium trails, illustrating an increase in ssGWAS resolution as more genotyped animals are included in the analyses. As previously shown, especially for populations with a small effective population size ( $N_e$ ) and more polygenic traits, increasing the genotype set reduces the estimation error and the shrinkage of SNP effects, which increases the power of discovering significant variants [34, 40, 41]. The benefit of an increase in the genotype set size can also be observed when comparing Approx\_GinvAPY with Approx\_GinvAPY450K. In general, for significant SNPs identified on chromosomes 7 and 20, the magnitude of p-values on the logarithmic scale obtained with Approx\_GinvAPY450K increased by 50% relative to results from Approx\_GinvAPY.

In the first set of analyses, when the same amount of data was used, an increase in noise was observed with Approx\_GinvAPY compared to Exact\_GinvAPY (Fig. 1, Additional file 1: Figures S1 and S2). However, when more genotyped animals were included with Approx\_GinvAPY450K, significant SNPs without a clear linkage disequilibrium pattern were no longer observed in all replicates (Fig. 3). This suggests that the benefit of increasing the genotype set overcomes the noise associated with an approximation that relies on APY and  $C^{u_2c u_2c_{approx}}$  and mitigates potential false positive associations. While evaluating two simulated populations with the same  $N_e$ , Misztal et al. [34] observed that increasing the number of individuals contributing with genotypes and phenotypes by three times increased the correct identification of significant SNPs. Similarly, Jang et al. [40] showed that for highly polygenic traits (2000 QTN) with an  $N_e$  of 20 and a moderate heritability of 0.30, no QTN was accurately

identified until a complete genotype set, composed of 30K genotyped animals, was included in the analyses. For livestock populations with even smaller  $N_e$  and traits of lower heritability, such as reproduction and fitness traits, QTN identification may be even more challenging, especially when limitations exist on the amount of genomic information used in the estimation process.

Total wall-clock time for the calculation of p-values with Approx\_GinvAPY450K was, on average, 24.47h, which was divided into building  $\mathbf{G}_{\text{APY}}^{-1}$  and saving components of  $\mathbf{A}_{22}^{-1}$  (6.6h), estimation of breeding values (6.67h), estimation of  $\mathbf{C}^{\text{u}_2\text{c}\text{u}_2\text{c}\text{approx}}$  (0.38h), and backsolving GEBV to SNP effects and approximation of  $\text{var}(\hat{\mathbf{a}}_i)$ . The entire process required no more than 87.64GB of RSS memory (Table 4). In comparison with the same method using a reduced set of genotyped animals in the first set of analyses (i.e., Approx\_GinvAPY), the increase in wall-clock time was linear with the increase in the number of genotypes included added, which was approximately nine times. However, the increase in RSS memory requirement was only five times.

The efficiency of the proposed approximation method (i.e., Approx\_GinvAPY) is because  $\text{var}(\hat{\mathbf{a}}_i)$  computations rely only on the genotypes of core animals, meaning that the computational requirement of inverting  $\mathbf{G}$  in Exact\_Ginv and obtaining  $\mathbf{G}_{\text{APY}}^{-1}$  in Exact\_GinvAPY is reduced to inverting a small matrix of relationships between core animals ( $\mathbf{G}_{\text{cc}}$ ) [16].

The optimal dimension of  $\mathbf{G}_{\text{cc}}$  is approximately a linear function of  $N_e$  of the population and should not be more than 15K for most livestock species or breeds [21, 22]. Moreover, with the Approx\_GinvAPY method, no inversion of the LHS is required. Instead,  $\mathbf{C}^{\text{u}_2\text{c}\text{u}_2\text{c}\text{approx}}$  are obtained accurately with a lower computational cost by a block sparse inversion of  $\mathbf{G}_{\text{APY}}^{-1}$  that had weights (effective

record contributions;  $\mathbf{D}$  in Eq. [9]) added to its diagonal [18]. Additionally, because Approx\_GinvAPY does not require the direct inversion of the LHS, efficient solvers such as PCG can be used in combination with the block implementation of APY, efficiently exploiting the sparseness of  $\mathbf{G}_{\text{APY}}^{-1}$  [36, 37].

Even though this study focuses on combining APY and  $\mathbf{C}^{\text{u}_2\text{c}\text{u}_2\text{c}\text{approx}}$  [18], any efficient method to approximate the GEBV prediction error covariance or SNP prediction error variances in large genotyped populations could be applied here. For a comparison of APY against other methods, we refer the reader to Bermann et al. [18] and Zaabza et al. [42].

Altogether, our results show that the current computational limitations for obtaining p-values for populations with many genotyped animals should no longer be an issue with the Approx\_GinvAPY method. The possibility of computing SNP p-values for those large genotyped populations should increase the power of detection of true variants and prevent future findings of ssGWAS from solely relying on SNP effects and variance explained by SNPs [7, 11]. It is worth noting that the results presented herein are based on a single-trait model in a purebred population. However, as long as reliabilities from more complex models and on populations with more complex breeding structures are accurately estimated, we expect that p-values will also be accurately approximated.

## Conclusions

The same genomic regions on chromosomes 7 and 20 were identified with p-values obtained with  $\mathbf{G}^{-1}$ ,  $\mathbf{G}_{\text{APY}}^{-1}$ , and the approximation based on  $\mathbf{G}_{\text{APY}}^{-1}$  with a reduced dataset, indicating the soundness of the proposed p-value computing method. Even though p-values were similar between computing methods, computational requirements for the new method were considerably reduced. When the approximation based on  $\mathbf{G}_{\text{APY}}^{-1}$  was applied to a genotyped population with almost half a million genotyped animals, SNPs on chromosomes 7 and 20 had stronger signals, and two new regions on chromosomes 6 and 14 were uncovered, indicating an increase in ssGWAS detection power when more genotypes are included in the analyses. Obtaining p-values in ssGWAS for such a large genotyped population required 24h, which is expected to increase linearly with the addition of noncore genotyped individuals. With a combination of APY and an approximation of the variance of estimated SNP effects, ssGWAS with p-values becomes computationally feasible for large genotyped populations.

**Table 4** Elapsed wall-clock time and Resident Set Size (RSS) requirements for p-values computation with Approx\_GinvAPY450K<sup>a</sup>

Software	Elapsed time, h:min	SD	Peak of memory, GB <sup>b</sup>	SD
PREGSF90	6:36	0:13	51.37	0.00
BLUPF90IOD3	6:40	0:31	43.82	0.00
ACCF90GS2	0:23	0:02	87.64	0.00
POSTGSF90	10:48	0:40	59.43	0.87
Total/Max	24:28		87.64	

<sup>a</sup> SNP p-values obtained from a data set of 450K genotyped animals with  $\mathbf{G}_{\text{APY}}^{-1}$  and  $\mathbf{C}^{\text{u}_2\text{c}\text{u}_2\text{c}\text{approx}}$  (Approx\_GinvAPY)

<sup>b</sup> Resident Set Size (RSS) memory. Values are displayed as average and standard deviations between three replicates

## Supplementary Information

The online version contains supplementary material available at <https://doi.org/10.1186/s12711-024-00925-3>.

**Additional file 1:** Figure S1. Manhattan plots for all p-value computing methods with a reduced data set in replicate 2. Single-step genome-wide association study for post-weaning weight with p-values obtained from a data set of 50K genotyped animals with (A)  $\mathbf{G}^{-1}$  and  $\mathbf{C}^{u_2u_2}$  (Exact\_Ginv), (B)  $\mathbf{G}_{APY}^{-1}$  and  $\mathbf{C}^{u_2c\ u_2c}$ (Exact\_GinvAPY), and (C)  $\mathbf{G}_{APY}^{-1}$  and  $\mathbf{C}^{u_2c\ u_2c\ approx}$ (Approx\_GinvAPY) in replicate 2; SNPs highlighted in green represent the three most significant SNP in the two peaks found with Exact\_Ginv (benchmark). Figure S2. Manhattan plots for all p-value computing methods with a reduced data set in replicate 3. Single-step genome-wide association study for post-weaning weight with p-values obtained from a data set of 50K genotyped animals with (A)  $\mathbf{G}^{-1}$  and  $\mathbf{C}^{u_2u_2}$  (Exact\_Ginv), (B)  $\mathbf{G}_{APY}^{-1}$  and  $\mathbf{C}^{u_2c\ u_2c}$ (Exact\_GinvAPY), and (C)  $\mathbf{G}_{APY}^{-1}$  and  $\mathbf{C}^{u_2c\ u_2c\ approx}$ (Approx\_GinvAPY) in replicate 3; SNPs highlighted in green represent the three most significant SNP in the two peaks found with Exact\_Ginv (benchmark). Figure S3. QQ plots for all p-value computing methods with a reduced data set in replicate 2. QQ plots for p-values obtained from a data set of 50K genotyped animals with (A)  $\mathbf{G}^{-1}$  and  $\mathbf{C}^{u_2u_2}$  (Exact\_Ginv), (B)  $\mathbf{G}_{APY}^{-1}$  and  $\mathbf{C}^{u_2c\ u_2c}$  (Exact\_GinvAPY), and (C)  $\mathbf{G}_{APY}^{-1}$  and  $\mathbf{C}^{u_2c\ u_2c\ approx}$ (Approx\_GinvAPY) in replicate 2. Figure S4. QQ plots for all p-value computing methods with a reduced data set in replicate 3. QQ plots for p-values obtained from a data set of 50K genotyped animals with (A)  $\mathbf{G}^{-1}$  and  $\mathbf{C}^{u_2u_2}$  (Exact\_Ginv), (B)  $\mathbf{G}_{APY}^{-1}$  and  $\mathbf{C}^{u_2c\ u_2c}$ (Exact\_GinvAPY), and (C)  $\mathbf{G}_{APY}^{-1}$  and  $\mathbf{C}^{u_2c\ u_2c\ approx}$ (Approx\_GinvAPY) in replicate 3.

### Acknowledgements

We thank the American Angus Association (St. Joseph, MO) for conceding the dataset used in this study.

### Author contributions

NGL, MB, IM, and DL, conceived and designed the study. NGL analyzed the data and wrote the first draft of the manuscript. MB made software modifications. All authors provided critical insights and revised the manuscript. All authors read and approved the final manuscript.

### Funding

This study was partially funded by Agriculture and Food Research Initiative Competitive Grant no. 2020-67015-31030 from the US Department of Agriculture's National Institute of Food and Agriculture.

### Availability of data and materials

The data supporting the findings of this study were provided from the American Angus Association (St. Joseph, MO) but restrictions apply to the availability of these data, which were used under license for the current study, and thus are not publicly available. The methods described here when using  $\mathbf{G}^{-1}$  and  $\mathbf{G}_{APY}^{-1}$  are included in BLUPF90+ and POSTGSf90, available at <http://nce.ads.uga.edu/software/>. The methods described here when using the approximation based on  $\mathbf{G}_{APY}^{-1}$  are included in BLUP90IOD3 and ACCF90GS, which are only available under research agreement with the Animal Breeding and Genetics group at UGA (<http://nce.ads.uga.edu/>).

### Declarations

#### Ethics approval and consent to participate

Not applicable.

#### Consent for publication

Not applicable.

### Competing interests

The authors declare that they have no competing interests.

Received: 6 November 2023 Accepted: 24 July 2024

Published online: 22 August 2024

### References

- Lourenco DAL, Tsuruta S, Fragomeni BO, Masuda Y, Aguilar I, Legarra A, et al. Genetic evaluation using single-step genomic best linear unbiased predictor in American Angus. *J Anim Sci*. 2015;93:2653–62.
- Tsuruta S, Lawlor TJ, Lourenco DAL, Misztal I. Bias in genomic predictions by mating practices for linear type traits in a large-scale genomic evaluation. *J Dairy Sci*. 2021;104:662–77.
- Abdollahi-Arpanahi R, Lourenco D, Misztal I. A comprehensive study on size and definition of the core group in the proven and young algorithm for single-step GBLUP. *Genet Sel Evol*. 2022;54:34.
- Misztal I, Lourenco D, Legarra A. Current status of genomic evaluation. *J Anim Sci*. 2020;98:skaa101.
- VanRaden PM. Efficient methods to compute genomic predictions. *J Dairy Sci*. 2008;91:4414–23.
- Strandén I, Garrick D. Derivation of equivalent computing algorithms for genomic predictions and reliabilities of animal merit. *J Dairy Sci*. 2009;92:2971–5.
- Wang H, Misztal I, Aguilar I, Legarra A, Muir WM. Genome-wide association mapping including phenotypes from relatives without genotypes. *Genet Res*. 2012;94:73–83.
- Misztal I, Wang H, Aguilar I, Legarra A, Tsuruta S, Lourenco D, et al. GWAS using ssGBLUP. In: *Proceedings of the 10th World Congress on Genetics Applied to Livestock Production: 17–22 August; Vancouver*. 2014.
- Fragomeni BDO, Misztal I, Lourenco DL, Aguilar I, Okimoto R, Muir WM. Changes in variance explained by top SNP windows over generations for three traits in broiler chicken. *Front Genet*. 2014;5:332.
- Wang H, Misztal I, Aguilar I, Legarra A, Fernando RL, Vitezica Z, et al. Genome-wide association mapping including phenotypes from relatives without genotypes in a single-step (ssGWAS) for 6-week body weight in broiler chickens. *Front Genet*. 2014;5:134.
- Aguilar I, Legarra A, Cardoso F, Masuda Y, Lourenco D, Misztal I. Frequentist p-values for large-scale-single step genome-wide association, with an application to birth weight in American Angus cattle. *Genet Sel Evol*. 2019;51:28.
- Gualdrón Duarte JL, Cantet RJ, Bates RO, Ernst CW, Raney NE, Steibel JP. Rapid screening for phenotype-genotype associations by linear transformations of genomic evaluations. *BMC Bioinformatics*. 2014;15:1–11.
- Bernal Rubio YL, Gualdrón Duarte JL, Bates R, Ernst C, Nonneman D, Rohrer G, et al. Meta-analysis of genome-wide association from genomic prediction models. *Anim Genet*. 2016;47:36–48.
- Lu Y, Vandehaar M, Spurlock D, Weigel K, Armentano L, Connor E, et al. Genome-wide association analyses based on a multiple-trait approach for modeling feed efficiency. *J Dairy Sci*. 2018;101:3140–54.
- Misztal I, Legarra A, Aguilar I. Using recursion to compute the inverse of the genomic relationship matrix. *J Dairy Sci*. 2014;97:3943–52.
- Bermann M, Lourenco D, Forneris NS, Legarra A, Misztal I. On the equivalence between marker effect models and breeding value models and direct genomic values with the Algorithm for Proven and Young. *Genet Sel Evol*. 2022;54:52.
- Misztal I, Wiggans G. Approximation of prediction error variance in large-scale animal models. *J Dairy Sci*. 1988;71:27–32.
- Bermann M, Lourenco D, Misztal I. Efficient approximation of reliabilities for single-step genomic best linear unbiased predictor models with the Algorithm for Proven and Young. *J Anim Sci*. 2022;100:skab353.
- Vitezica Z, Aguilar I, Misztal I, Legarra A. Bias in genomic predictions for populations under selection. *Genet Res*. 2011;93:357–66.
- García ALS, Masuda Y, Tsuruta S, Miller S, Misztal I, Lourenco D. Indirect predictions with a large number of genotyped animals using the algorithm for proven and young. *J Anim Sci*. 2020;98:skaa154.
- Cesarani A, Lourenco D, Tsuruta S, Legarra A, Nicolazzi E, VanRaden P, et al. Multibreed genomic evaluation for production traits of dairy cattle in the

- United States using single-step genomic best linear unbiased predictor. *J Dairy Sci.* 2022;105:5141–52.
22. Pocrnic I, Lourenco DA, Masuda Y, Legarra A, Misztal I. The dimensionality of genomic information and its effect on genomic prediction. *Genetics.* 2016;203:573–81.
  23. VanRaden P, Freeman A. Rapid method to obtain bounds on accuracies and prediction error variances in mixed models. *J Dairy Sci.* 1985;68:2123–33.
  24. Strandén I, Mäntysaari E. Comparison of some equivalent equations to solve single-step GBLUP. In: *Proceedings of the 10th World Congress on Genetics Applied to Livestock Production.* 17–22 August 2014; Vancouver. 2014.
  25. Misztal I, Tsuruta S, Lourenco D, Aguilar I, Legarra A, Vitezica Z. Manual for BLUPF90 family of programs; 2014. [http://nce.ads.uga.edu/wiki/lib/exe/fetch.php?media=blupf90\\_all8.pdf](http://nce.ads.uga.edu/wiki/lib/exe/fetch.php?media=blupf90_all8.pdf). Accessed 15 Oct 2023.
  26. Aguilar I, Misztal I, Johnson D, Legarra A, Tsuruta S, Lawlor T. Hot topic: a unified approach to utilize phenotypic, full pedigree, and genomic information for genetic evaluation of Holstein final score. *J Dairy Sci.* 2010;93:743–52.
  27. Bradford HL, Pocrnić I, Fragomeni BO, Lourenco DAL, Misztal I. Selection of core animals in the Algorithm for Proven and Young using a simulation model. *J Anim Breed Genet.* 2017;134:545–52.
  28. Pocrnic I, Lourenco DA, Chen C-Y, Herring WO, Misztal I. Crossbred evaluations using single-step genomic BLUP and algorithm for proven and young with different sources of data. *J Anim Sci.* 2019;97:1513–22.
  29. Lourenco D, Tsuruta S, Aguilar I, Masuda Y, Bermann M, Legarra A, et al. Recent updates in the BLUPF90 software suite. In: *Proceedings of 12th World Congress on Genetics Applied to Livestock Production: 3–8 July; Rotterdam.* 2022.
  30. Legarra A, Christensen OF, Aguilar I, Misztal I. Single Step, a general approach for genomic selection. *Livest Sci.* 2014;166:54–65.
  31. Mancin E, Lourenco D, Bermann M, Mantovani R, Misztal I. Accounting for population structure and phenotypes from relatives in association mapping for farm animals: a simulation study. *Front Genet.* 2021;12: 642065.
  32. Devlin B, Roeder K. Genomic control for association studies. *Biometrics.* 1999;55:997–1004.
  33. Hidalgo J, Lourenco D, Tsuruta S, Masuda Y, Miller S, Bermann M, et al. Changes in genomic predictions when new information is added. *J Anim Sci.* 2021;99:skab004.
  34. Misztal I, Lourenco D, Pocrnic I. SNP profile for quantitative trait nucleotide in populations with small effective size and its impact on mapping and genomic predictions. *bioRxiv.* 2023. <https://doi.org/10.1101/2023.02.16.528829>.
  35. Misztal I. Inexpensive computation of the inverse of the genomic relationship matrix in populations with small effective population size. *Genetics.* 2016;202:401–9.
  36. Masuda Y, Misztal I, Tsuruta S, Legarra A, Aguilar I, Lourenco DAL, et al. Implementation of genomic recursions in single-step genomic best linear unbiased predictor for US Holsteins with a large number of genotyped animals. *J Dairy Sci.* 2016;99:1968–74.
  37. Junqueira VS, Lourenco D, Masuda Y, Cardoso FF, Lopes PS, Silva FFE, et al. Is single-step genomic REML with the algorithm for proven and young more computationally efficient when less generations of data are present? *J Anim Sci.* 2022;100:skac082.
  38. Garcia A, Miller S, Tsuruta S, Lourenco D, Misztal I, Lu D, et al. Updating the core animals in the algorithm for proven and young in the American Angus Association national evaluations. In: *Proceedings of 12th World Congress on Genetics Applied to Livestock Production (WCGALP) Technical and species orientated innovations in animal breeding, and contribution of genetics to solving societal challenges;* 2022.
  39. Vandenplas J, Calus MP, ten Napel J. Sparse single-step genomic BLUP in crossbreeding schemes. *J Anim Sci.* 2018;96:2060–73.
  40. Jang S, Tsuruta S, Leite NG, Misztal I, Lourenco D. Dimensionality of genomic information and its impact on genome-wide associations and variant selection for genomic prediction: a simulation study. *Genet Sel Evol.* 2023;55:49.
  41. Lourenco D, Fragomeni B, Bradford H, Menezes I, Ferraz J, Aguilar I, et al. Implications of SNP weighting on single-step genomic predictions for different reference population sizes. *J Anim Breed Genet.* 2017;134:463–71.
  42. Zaabza HB, Van Tassell CP, Vandenplas J, VanRaden P, Liu Z, Eding H, et al. Invited review: Reliability computation from the animal model era to the single-step genomic model era. *J Dairy Sci.* 2023;106:1518–32.

### Publisher's Note

Springer Nature remains neutral with regard to jurisdictional claims in published maps and institutional affiliations.